

# KINETIC MONTE CARLO BASED CATALYTIC VISCOUS WALL BOUNDARY MODELING IN CFD SIMULATION OF HIGH-ENTHALPY NON-EQUILIBRIUM FLOW

Qin Li<sup>1,2</sup>, Xiaofeng Yang<sup>2</sup>, Wei Dong<sup>1</sup> & Yanxia Du<sup>2</sup>

<sup>1</sup>School of Mechanical Engineering, Shanghai Jiao Tong University, China <sup>2</sup>State Key Laboratory of Aerodynamics, China Aerodynamics Research and Development Center, China

### **Abstract**

Heterogeneous catalytic reactions between dissociated atoms after the shockwave and thermal protective materials can lead to a significant part of aerodynamic heating on the surface of high-speed aircraft. A kinetic Monte Carlo (KMC) based catalytic model simulating four-step heterogeneous catalysis was constructed and was coupled into computational fluid dynamics (CFD) method as catalytic viscous wall boundary by interpolation. The KMC-embedded CFD simulation method aimed at involving microscale reaction kinetics in CFD simulation, further obtaining heat transfer rate with physical basis on chemical reacting gas-solid interface. Local aerothermal environment calculated from a self-developed CFD solver provided thermochemical parameters for the KMC method. The output of KMC, namely the recombination coefficient of atoms, was used as a catalytic viscous wall boundary condition in the CFD solver. The accuracy of KMC method in predicting recombination coefficient, the effectiveness of the self-developed CFD solver in simulating chemical reacting gas flow, and the ability of the KMC-embedded CFD method in calculating heat transfer rate was verified. The results showed that simulation of high-enthalpy flow with the current method could drive a deterministic heat transfer rate on the surface of high-speed aircraft, thus improving the reliability of aerodynamic heating prediction on thermal protection material.

**Keywords:** high enthalpy flow, aerodynamic heating, gas-solid interface, heterogeneous catalysis, kinetic Monte Carlo method

### 1. Introduction

When aircraft flying at an altitude of 20-60 km with a Mach number greater than 10, the air in front of the aircraft nose will be heated higher than 5000K, and the aircraft surface will withstand harsh aerodynamic heating[1]. Part of the molecules dissociate into atoms after the shock wave and part of the atoms in the shock layer recombine near the surface. When time scales of chemical reaction and gas flow are of the same magnitude, chemical non-equilibrium effect should be considered in simulation of a high enthalpy flow field and surface heat transfer rate[2]. The heterogeneous catalysis effect is remarkable on the interface of chemical non-equilibrium flow and thermal protection material [3]. Heterogeneous catalysis on high-speed aircraft surfaces means the recombination process of gas atoms can be accelerated due to the catalysis of solid thermal protection material. As a result, an amount of chemical energy will be released on the surface, increasing the heat transfer rate into the thermal protection system (TPS). Wind tunnel and flight experiments have proved that the catalysis effect can lead to a heat transfer rate difference of 2-4 times[4, 5], indicating that it cannot be ignored.

In the design of TPS, numerical simulation of heat transfer rate should be carried out to ensure safety. Surface catalysis effect has been included in Computational Fluid Dynamics (CFD) by two kinds of catalytic models. One is to specify net recombination coefficients of atomic species [6, 7], as constants or temperature-dependent Arrhenius expressions. Another is to specify the reaction rate for every reaction step of heterogeneous catalysis, which can be obtained from the reacting mechanism[8, 9]. To consider the dependency of catalysis and heat transfer rate on materials, many

experiments on metal, silica-based and carbon-based materials have been carried out and some material-related fitting expressions of catalytic coefficients have also been obtained [10-14].

With the development of high-performance computing and microscale numerical research methods. such as Molecular Dynamics (MD) and first principles simulation, new reaction kinetics were found. Norman et al. focused on the adsorption and recombination behavior of oxygen atoms on silicabased materials[15-17]. Valentini et al. emphasized the adsorption and dissociation of oxygen on platinum using ReaxFF [18, 19]. Buchachenko et al. studied rates of elementary reaction steps on thermal protective surfaces by first principles simulation [20-22]. Cui et al. analyzed the competing effects between catalysis and ablation reactions on carbon-based material[23]. These achievements contribute to revealing reaction trajectories and accumulating rate-related parameters from a micro perspective, further providing a mechanism basis for the construction of meso/macro-scale models. In recent years, the kinetic Monte Carlo (KMC) method has been widely used in surface reaction simulation for its advantages of accuracy in spatial scale and efficiency in time consumption [24, 25]. KMC has been acknowledged to be a mesoscale method to bridge the scaling gap between microscopic and macroscopic material simulation[26]. General or specially used codes have been developed to simulate surface reaction processes, such as KMCLib by Mikael[27, 28], kmos by Hoffmann[29], MonteCoffee by Jørgensen[30] and Dooling's method[31]. As a typical kind of surface chemical reaction, heterogeneous catalysis has also been simulated by the KMC method in chemical engineering[32]. Guerra[33] studied the recombination of nitrogen atoms on a silica surface using Fichthorn's KMC method[34]. Schaefer simulated the transport of fluid in the chemical reactor by coupling the CFD and KMC methods [35]. Many first-principle KMC researches have been done to simulate the recombination of CO and O on the RuO2 surface[36-38]. The KMC method has been proven to help reveal the statistical character of surface reactions. However, most KMC simulations of catalysis have been done to find more efficient catalysts [39], for better performance in chemical production, such as better catalytic converters for gasoline vehicles [26]. Research work to model heterogeneous catalysis reactions on viscous walls of high-speed aircraft using KMC is scarce. Thoemel et al.[40] focused on the catalysis of high enthalpy CO<sub>2</sub> flow on aircraft surfaces and found the non-random distribution of dissociated species on surface adsorption sites. KMC-based catalytic models have rarely been used in aerodynamic heating prediction on aircraft.

The present study developed KMC simulation codes specific for the four-step heterogeneous catalysis process and coupled this KMC-based catalytic model into a CFD solver, CAPTER [41]. Microscale gas-solid interaction parameters were obtained from literature data. By this KMC-embedded CFD method, microscopic physical information of heterogeneous catalysis can be involved in the macroscopic solution of the flow field. As a result, modeling of viscous wall boundary with heterogeneous catalysis effect can be supported by more intrinsic mechanisms, further improving the accuracy of aerodynamic heating prediction. Heat and mass transfer on a two-dimensional(2D) cylinder surface in high-speed airflow was simulated and analyzed using the KMC-embedded CFD method. Moreover, the time consumption of the KMC-embedded CFD calculation was also reported.

# 2. KMC Modeling of catalytic reaction in CFD simulation

### 2.1 CFD solver of chemical non-equilibrium flow

Governing equations of chemical non-equilibrium flow are Navier-Stokes equations, of which the source terms are caused by homogeneous chemical reactions in the shock layer. The variation of species mass fraction with time is caused by convection, diffusion and homogeneous chemical reaction

$$\frac{\partial \rho_{s}}{\partial t} = -\left(\frac{\partial \rho_{s} u}{\partial x} + \frac{\partial \rho_{s} v}{\partial y} + \frac{\partial \rho_{s} w}{\partial z}\right) + \frac{\partial}{\partial x}\left(\rho D_{s} \frac{\partial c_{s}}{\partial x}\right) + \frac{\partial}{\partial y}\left(\rho D_{s} \frac{\partial c_{s}}{\partial y}\right) + \frac{\partial}{\partial z}\left(\rho D_{s} \frac{\partial c_{s}}{\partial z}\right) + S_{s}$$

$$\tag{1}$$

where s=1,2,...,N and N is the number of chemical species in the flow field. In Eq.(1),  $\rho_s$  and  $c_s$  are the specific density and mass fraction of species s respectively, u, v and w are velocity components in three directions x, y and z,  $D_s$  is the diffusion coefficient of species s, and  $S_s$  is the source term caused by homogeneous chemical reactions in the flow filed near to the viscous wall. Homogeneous chemical reactions of gas molecules and dissociated atoms in the shock layer can be characterized by gas models, to which Park [42], Gupta [43] and Kim [44] have made quite a

contribution. Present Navier-Stokes equations solver, CAPTER, adopted a 5-reaction of 5-species gas model. Details of CAPTER and gas model can be found in the authors' previous work [9, 45, 461.

# 2.2 Reaction kinetics of heterogeneous catalysis

The heterogeneous catalysis mechanism on high-speed aircraft surfaces was concluded from microscale research on chemical reacting kinetics. Four steps were considered in the present catalytic model, including chemical adsorption (Ad), Eley-Rideal (ER) recombination, Langmuir-Hinshelwood (LH) recombination and thermal desorption (Td) of adsorbed atoms. These four-step reactions above can be expressed as

$$A(g) + (s) \to A(s) \tag{2}$$

$$A(g) + A(s) \rightarrow A_2(g) + (s) \tag{3}$$

$$A(s) + A(s) \rightarrow A_2(g) + 2(s) \tag{4}$$

$$A(s) \to A(g) + (s) \tag{5}$$

where A and A<sub>2</sub> refer to a specified atom and a dual-atomic molecule, and (s) and (g) represent the surface adsorption phase and gas phase, respectively.

The reaction rate can be explained as the reaction number per site in unit time, of which the unit is 1/site · s . It is related to the collision frequency of atoms on every site and the reaction rate constant. Collision is decided by the thermal motion of atoms and its frequency can be calculated as

$$\varphi_{A} = \frac{\omega_{A} \times A_{V} \times \sqrt{\frac{k_{B}T_{W}}{2\pi M_{A}}}}{N_{S}}$$
 (6)

where  $\omega_{\rm A}$  is the molar concentration of A(g),  $A_{\rm V}$  is Avogadro constant,  $T_{\rm W}$  is wall temperature,  $k_{\rm B}$ is Boltzmann constant,  $\mathit{M}_{\mathrm{A}}$  is the weight of A and  $\mathit{N}_{\mathrm{S}}$  is the number density of adsorption sites on solid material. The reaction rate constant is related to the activation energy of every reaction step, which differs with materials and gas species. Normally, activation energies of adsorption and ER recombination are lower than those of LH recombination, while thermal desorption needs the highest activation energy.

For adsorption, the reaction rate  $r_{\mathrm{Ad}}$  is the product of adsorption rate constant  $k_{\mathrm{Ad}}$  and collision frequency

$$r_{\rm Ad} = k_{\rm Ad} \times \varphi_{\rm A} \tag{7}$$

Similar to that of adsorption, the reaction rate of ER recombination is the product of the ER recombination rate constant  $k_{ER}$  and collision frequency

$$r_{\mathsf{ER}} = k_{\mathsf{ER}} \times \varphi_{\mathsf{A}} \tag{8}$$

For LH recombination, reactants A(s) migrate between surface adsorption sites with a frequency of  $\varphi_{\rm M}$  , so its reaction rate can be written as

$$r_{\rm LH} = k_{\rm LH} \times \varphi_{\rm M} \tag{9}$$

Where  $k_{LH}$  is the rate constant of LH recombination, representing the probability of recombination when two adsorbed atoms migrate among adsorption sites. Special reacting nature has been found that LH recombination can only occur between two nearest neighbor sites[14]. The reaction rate of thermal desorption is determined by the thermal vibration frequency  $\varphi_{Td}$  of A(s) and the rate constant  $k_{\mathsf{Td}}$ .

$$r_{\mathsf{Td}} = k_{\mathsf{Td}} \times \varphi_{\mathsf{Td}} \tag{10}$$

All rate constants of the above four reaction steps are closely related to activation energy and wall temperature. Parameters of rate constant expressions have been acquired by experimental fitting or microscopic simulation and some have been adopted in aerodynamic heating prediction [47]. What's more, these four reaction steps are coupled together and it's difficult to describe the interaction of them in one analytical model. As a result, it is difficult to accurately predict the recombination coefficient, which is defined as the ratio of recombined atoms by total collided gas atoms, by theoretical method. Furthermore, uncertainty in the recombination coefficient will lead to indeterminacy in heat transfer rate prediction on thermal protective surfaces.

## 2.3 KMC modeling for heterogeneous catalysis

The KMC method selects a series of reaction events according to their rate constants and the number of sites that satisfy the requirements of reaction steps. Configuration (C) describes the state (occupied or vacant) of every surface adsorption site in the studied surface system, while coverage ( $\theta$ ) is the ratio of occupied site number to total site number. Based on the aforementioned reaction mechanism, a KMC-based catalytic model can be constructed by simulating the time evolution of surface configuration. Heterogeneous reaction steps occurring on certain sites will change the configuration.

The governing equation of the surface reaction system can be written as

$$\frac{dP_{\alpha}}{dt} = \sum_{\beta} (W_{\alpha\beta} P_{\beta} - W_{\beta\alpha} P_{\alpha}) \tag{11}$$

where  $P_{\alpha}$  is the probability of surface in configuration  $\alpha$ . Change of  $P_{\alpha}$  over time is determined by processes that can change other configurations to  $\alpha$  and processes that can change  $\alpha$  to other configurations, as well as their rates  $W_{\alpha\beta}$  and  $W_{\beta\alpha}$  [24]. KMC provides an approach to arrive a steady coverage by selecting a series of reactions, according to the occupied state of sites and reaction rates. Reaction step selection is essentially importance sampling, where site occupied state and reaction rate determine the possibility and probability respectively. The present KMC method to describe heterogeneous catalysis was developed from that of KMCLib [27, 28], by adding the nature of surface heterogeneous catalysis.

Gas-solid interaction parameters, such as adsorption site density and activation energies, can be well defined from electronic structure calculation, molecular dynamics (MD) method or experimental data. Besides of above parameters, two thermochemical parameters are necessary to get the recombination coefficient, including surface temperature and molar concentration of gas atoms near the surface. Based on these parameters, the evolution of surface configuration and reaction number of every step can be recorded. During evolution, recombination coefficients can be obtained by the time average of reaction numbers.

A two-dimensional (2D) lattice was adopted to map a catalytic surface system, where one lattice node represents one adsorption site. The procedure of KMC simulation on surface four-step heterogeneous catalysis is shown in Figure 1. The detailed steps are:

(1) According to the present surface configuration, count the number of sites  $N_i (1 \le i \le 4)$  that satisfy the condition for reaction step i to occur. The necessary surface occupied condition for every reaction step is listed in Table 1, which gives the criteria for whether a certain site is counted or not.

Table 1 Site occupied conditions for adsorption, ER/LH recombination and thermal desorption

Reaction type	Site occupied condition			
Adsorption	Vacant site			
ER recombination	Occupied site			
LH recombination	ation Two nearest neighbored occupied sites			
Thermal desorption	Occupied site			

<sup>(2)</sup> Based on rate constant related gas-surface interaction parameters and thermochemical conditions, the reaction rate  $r_i$  of reaction step i can be calculated using Eqs.(7-10). The total reaction rate  $R_i$  of reaction step i is defined as

$$R_i = r_i \times N_i \tag{12}$$

and represents the importance of reaction step i when selecting a reaction to occur by sampling. (3) Define  $p_i$  as the accumulated total reaction rate, as shown in Eq.(13). For a random number  $\rho_1$  in  $(0, p_4)$ , if  $\rho_1$  satisfies Eq.(14), then reaction step i is selected to be the type of next reaction.

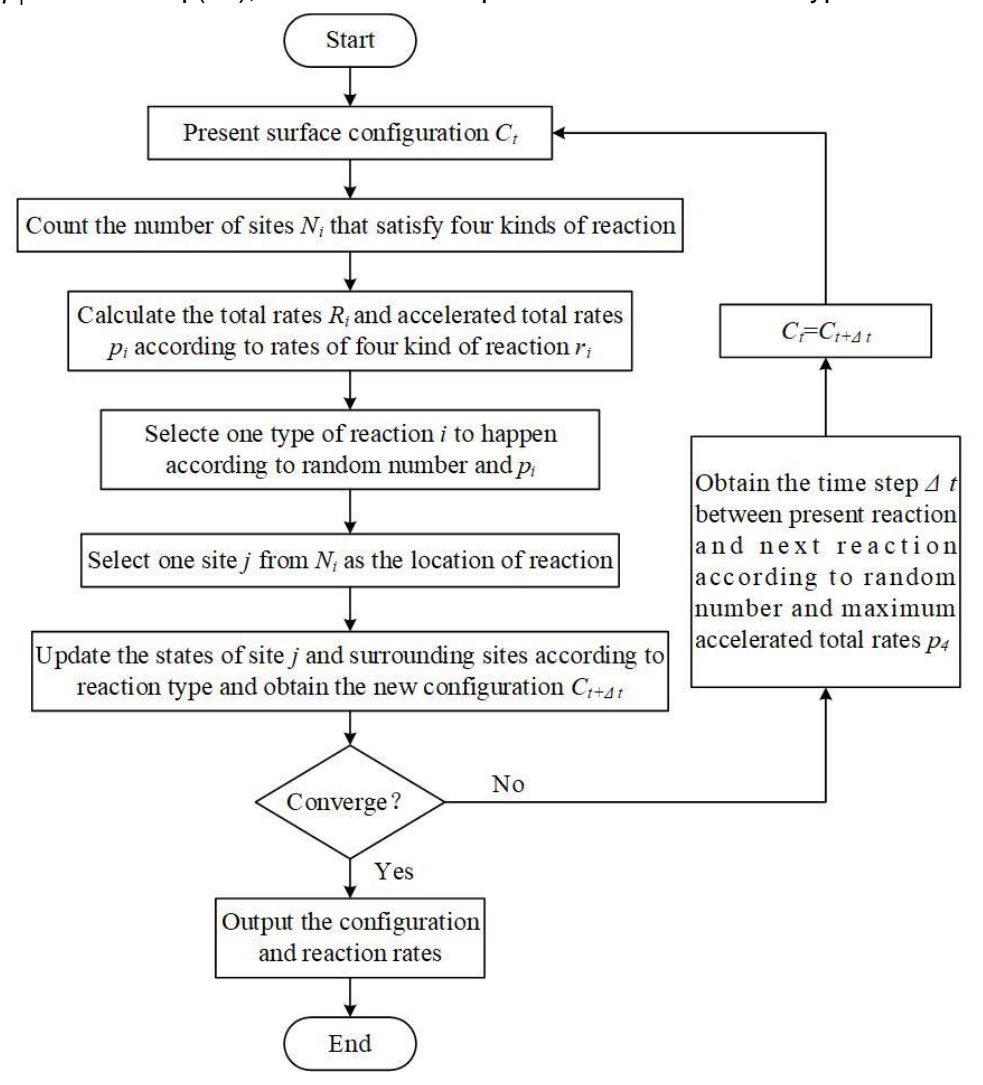


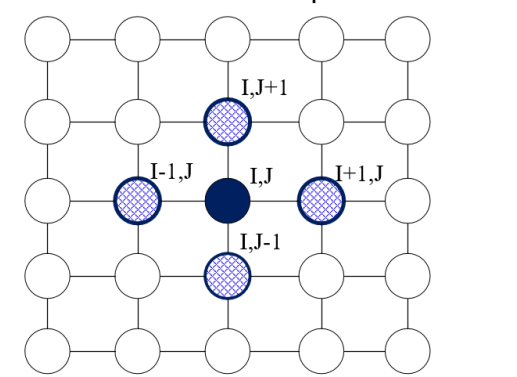
Figure 1 - Solution progress of KMC

$$p_i = \sum_{i=1}^i R_i \tag{13}$$

$$p_{i-1} < p_1 \le p_i \tag{14}$$

- (4) In  $N_i$  sites where reaction step i can take place, one specific site j among them is randomly selected to be the scene at this evolution.
- (5) Configuration update has been acknowledged as the most time-consuming process in KMC. To update the configuration locally, the occupied state of the target node itself and that of the nearest neighbors are stored in the description of every lattice node. That means to describe the state of one lattice node, the vacant or occupied states of present, left, right, top and bottom positions are labeled, as  $[s_{center}, s_{right}, s_{left}, s_{top}, s_{bottom}]$ . For adsorption, ER recombination and thermal desorption that occur on one adsorption site, the reaction changes the state of the center node and that of the four nearest neighbor nodes. As shown in Figure 2,  $s_{center}$  of node (I,J),  $s_{right}$  of node (I-1,J),  $s_{left}$  of node (I+1,J),  $s_{top}$  of node (I,J-1) and  $s_{bottom}$  of node (I,J+1) change from vacant to occupied when an atom is adsorbed on node (I,J). However, LH recombination changes states of eight nodes, as shown in Figure 3, because two nearest neighbor sites are involved in LH recombination. What's

more, a periodic condition was adopted on the lattice boundary in the simulation.



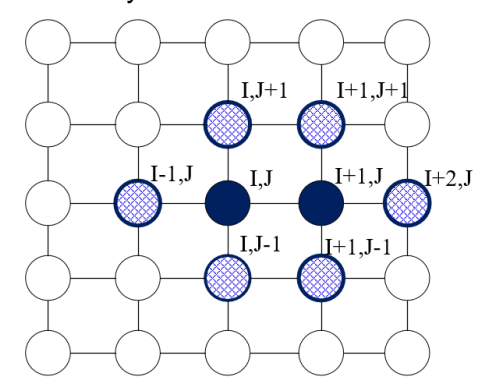


Figure 2 - Configuration description of a lattice node

Figure 3 - Lattice nodes influenced by LH recombination

(6) According to the last updated configuration, another selection of reaction step upon accumulated total rates is needed, until the recombination coefficient of atoms converges.

The main difference between kinetics-based catalytic models constructed by the KMC method and the macroscopic phenomenological method is located in the distribution assumption of adsorbed atoms. Macroscopic phenomenological models, which are also based on multi-step reaction theory, take the mean-field distribution of adsorbed atoms as a prerequisite. While KMC method can take spatial constraints into account during simulating surface configuration evolution, which is possible to result in the ununiform occupation of atoms on the surface.

In this KMC simulation specified for four-step heterogeneous catalysis, one restrictive condition was adopted: LH recombination could only occur between the two nearest neighbor sites. This nature of LH recombination has been found by microscopic research. Qualitatively, chemical bonds between adsorbed atoms and surface bulk atoms are strong and it's difficult for an adsorbed atom to break the bond and recombine with another distant adsorbed atom.

### 2.4 KMC-embedded CFD method

CFD method disperses Navier-Stokes equations in macroscopic space by grid nodes, while the KMC-based catalytic model calculates recombination coefficients of atomic species on atomic scale lattice under certain input parameters from macroscopic flow field. Therefore, KMC simulation can only be carried out at one grid node, using its local temperature and concentration condition as inputs. Gas-solid interaction parameters are specified in the KMC simulation. Invoking KMC simulation at every CFD grid node is computationally prohibitive, so an interpolation method is demanded to gain recombination coefficients of all CFD grid nodes by the limited number of KMC simulations, as shown in Figure 4.

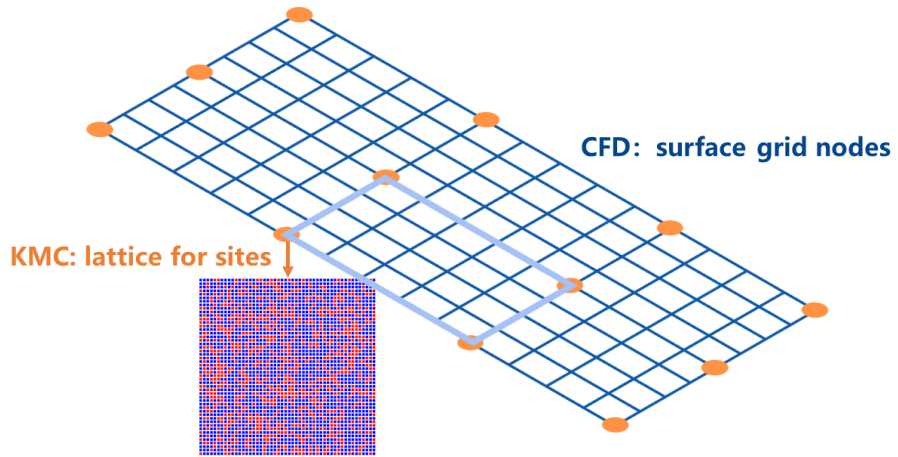


Figure 4 - CFD grid nodes of surface and limited number of nodes to operate KMC simulation. The bilinear interpolation method was adopted in the coupling of the CFD solver and the KMC-based catalytic model. After obtaining recombination coefficients of certain CFD nodes by KMC simulation, recombination coefficients of any CFD nodes that won't operate by KMC simulation can be calculated.

by this interpolation. Due to the 3-dimensional characteristics of aircraft surface and the 2-dimensional serviceability of bilinear interpolation, some extensions have been made to cater to the 3-dimensional surface.

As shown in Figure 5, the rectangle with blue solid lines represents a surface zone in the IJ plane of computational space in CFD and variable values ( $f_1 \sim f_4$ ) on its four vertices, ( $I_{\min}, J_{\min}, K$ ), ( $I_{\max}, J_{\min}, K$ ) and ( $I_{\max}, J_{\max}, K$ ), have been known. In the KMC-embedded CFD situation, f is recombination coefficient and can be calculated from KMC simulation. The purpose of this interpolation is to obtain f of any CFD grid node, (I, J, K), by  $f_1 \sim f_4$ . Detailed treatments are:

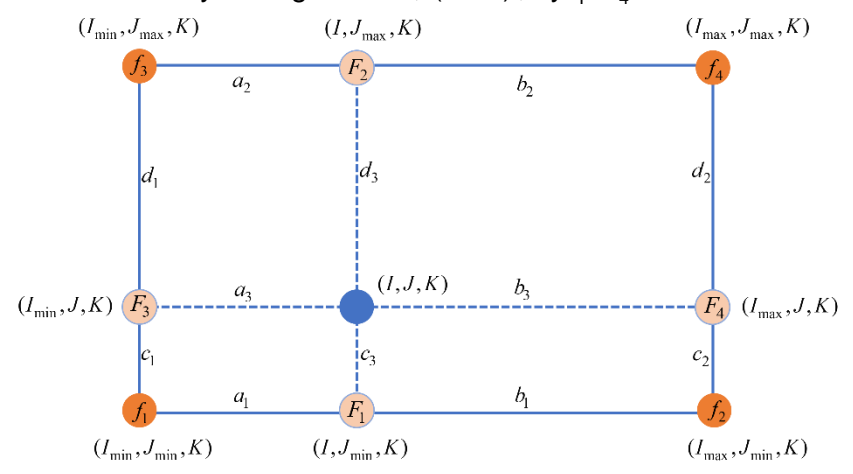


Figure 5 - Bilinear interpolation sketch using 4 values of vertices

- (1) Index coordinates of the projected grid nodes in four directions:  $(I_{\min}, J, K)$ ,  $(I_{\max}, J, K)$ ,  $(I, J_{\min}, K)$  and  $(I, J_{\max}, K)$ .
- (2) According to the computational space coordinates of nine nodes in Figure 5, obtain the coordinates of these nine nodes in physical space. Then calculate the Euclidean distances,  $a_1 \sim a_3$ ,  $b_1 \sim b_3$ ,  $c_1 \sim c_3$  and  $d_1 \sim d_3$ , by

$$d = \sqrt{\Delta x^2 + \Delta y^2 + \Delta z^2} \tag{15}$$

(3) Values of four projected nodes  $F_1 \sim F_4$  can be calculated by linear interpolations of endpoint nodes on corresponding edges.

$$\begin{cases} F_{1} = \frac{b_{1}}{a_{1} + b_{1}} \cdot f_{1} + \frac{a_{1}}{a_{1} + b_{1}} \cdot f_{2} \\ F_{2} = \frac{b_{2}}{a_{2} + b_{2}} \cdot f_{3} + \frac{a_{2}}{a_{2} + b_{2}} \cdot f_{4} \\ F_{3} = \frac{c_{1}}{c_{1} + d_{1}} \cdot f_{3} + \frac{d_{1}}{c_{1} + d_{1}} \cdot f_{1} \\ F_{4} = \frac{c_{2}}{c_{2} + d_{2}} \cdot f_{4} + \frac{d_{2}}{c_{2} + d_{2}} \cdot f_{2} \end{cases}$$

$$(16)$$

(4) A second linear interpolation between  $F_1$  and  $F_2$  is carried out by

$$R_1 = \frac{d_3}{c_3 + d_3} \times F_1 + \frac{c_3}{c_3 + d_3} \times F_2 \tag{17}$$

And similar operation is taken to interpolate  $F_3$  and  $F_4$ 

$$R_2 = \frac{b_3}{a_3 + b_3} \times F_3 + \frac{a_3}{a_3 + b_3} \times F_4 \tag{18}$$

(5) Finally, the average of  $R_1$  and  $R_2$  is selected to be the value of node (I,J,K)

$$f = \frac{1}{2} \times R_1 + \frac{1}{2} \times R_2 \tag{19}$$

The recombination coefficient of atomic species A,  $\gamma_A$ , on the surface participates in the CFD calculation as boundary conditions on the interface between chemical reacting gas flow and viscous wall. Diffusion mass flux (left term in Eq. (20)) of A and catalytic reacting mass flux (right term in Eq. (20)) are balanced at a steady state. In Eq. (20),  $D_A$  represents the diffusion coefficient and  $\frac{\partial \omega_A}{\partial n}$  is the molarity gradient in the normal direction of the wall.

$$-D_{A}\frac{\partial \omega_{A}}{\partial n} = \gamma_{A}\omega_{A} \tag{20}$$

KMC-embedded CFD simulation of the chemical non-equilibrium flow field and surface heterogeneous catalysis operates as Figure 6. Based on thermochemical conditions from CFD simulation, recombination coefficients can be obtained by the KMC method. Furthermore, recombination coefficients will be considered in the viscous wall boundary condition of the next CFD iteration. By this, surface heat transfer rates Q, including convective and catalytic heat transfer rates, will converge with the iteration gradually.

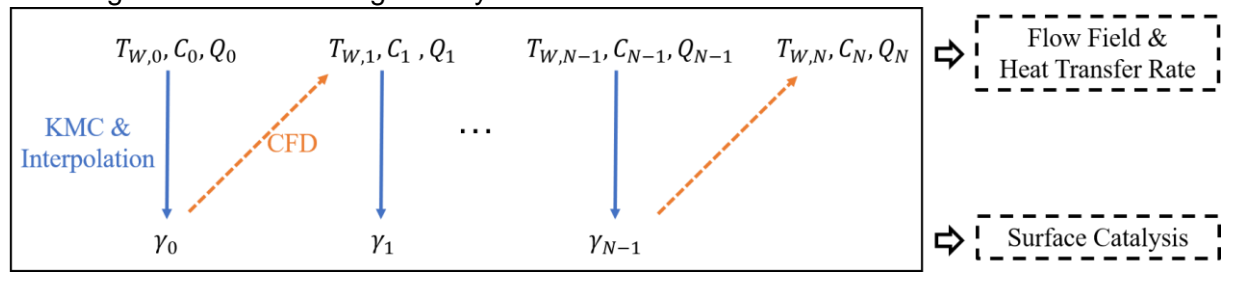


Figure 6 - Operation of KMC-embedded CFD simulation on flow field and surface catalysis

### 3. Verification of Methods

### 3.1 Verification of KMC method

Before being embedded into the CFD solver, the KMC algorithm should be verified to be effective in predicting recombination coefficients of atoms on given materials, with the property parameters provided. Firstly, independency validation on lattice size is necessary for KMC simulation. Reactions on several nodes will lead to large fluctuation of surface coverage if the number of total lattice nodes is not enough, while too large number of total lattice nodes would result in high time consumption. Four cases, whose lattice sizes were 10\*10, 20\*20, 40\*40 and 80\*80 respectively, were tested by fluctuation of recombination coefficients during time evolution. The initial lattice configuration of each case was vacant, meaning that there was no pre-adsorbed atom on the surface. There will be more reactions during the same period on larger lattices. To keep a similar physical time scale among different cases, the number of total reactions ( $n_{\rm total}$ ) and interval number of reactions ( $\Delta n$ ) to obtain recombination coefficients by averaging should be proportional to the number of lattice nodes.  $n_{\rm total}$  and  $\Delta n$  of above four cases are listed in Table 2. The time cost for every case using the same computer was also given. Computation was performed serially using the Intel i7-8700 CPU @ 3.20GHz processor.

Table 2 KMC case settings of different lattice sizes

Table 2 1 and dates detailings of annothing and actions					
Lattice size	$\emph{n}_{ ext{total}}$	$\Delta n$	Time cost (s)		
10*10	50,000	1,250	1.3		
20*20	200,000	5,000	15.2		
40*40	800,000	20,000	209.5		
80*80	3,200,000	80,000	3,495.7		

Figure 7 presents the fluctuation of recombination coefficients with time in KMC simulation. It can be concluded from Figure 7 that with the increase in lattice size, the recombination coefficient under the same species concentration and surface temperature condition predicted by the KMC method is more stable. However, as shown in Table 2, time consumption sharply increases with lattice size. Computational time cost increases to about 16 times as the number of lattice nodes doubles. This is

because both the time consumption for selecting a single reaction and the number of reactions (or the number of selections) increase rapidly with lattice size. In consideration of both accuracy and efficiency, lattice size 40\*40 was selected to be coupled into the CFD boundary condition in the present study.

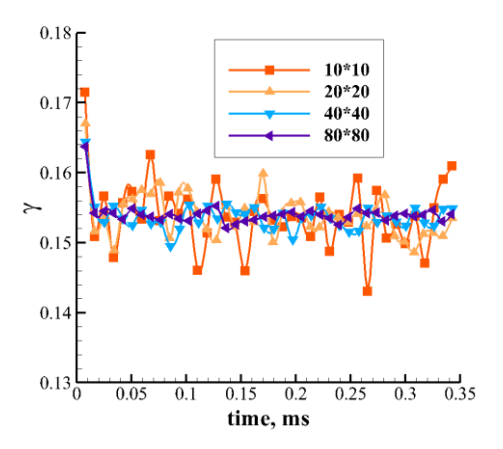
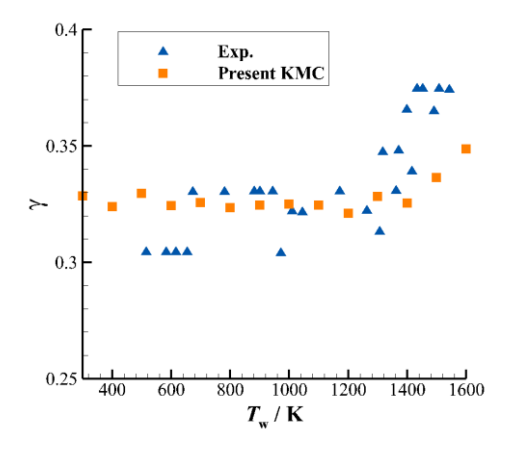


Figure 7 - Recombination coefficient fluctuation with time under different lattice sizes Separated KMC simulation of specified atoms on certain surfaces was also based on a 40\*40 lattice. The catalysis phenomenon is remarkable on metal surfaces, such as copper (Cu), nickel (Ni), platinum (Pt) and tungsten (W). Barbato [48] summarized gas-solid interaction parameters related to reaction rate constants of catalytic reaction steps on these metal materials, which were also adopted to calculate heat transfer rates on metal and SiO2 surfaces [49]. These parameters were obtained from experimental data and showed high accuracy[48]. For such reasons, these parameters were adopted to calculate the reaction rates of four-step reactions on the Pt and W surfaces in the present KMC simulation.

The recombination coefficients obtained from the present KMC simulation were compared with those of the reactor experiment measurement [50]. Figure 8 and Figure 9 give the recombination coefficients of nitrogen atoms on Pt and W surfaces respectively. Compared with the experimental data, the maximum relative error of KMC calculated  $\gamma_N$  is about 10% for the Pt surface.  $\gamma_N$  on W surface is also in good agreement with experimental results under high surface temperatures. The above comparison indicates the high accuracy of the present KMC method for heterogeneous catalysis when material-gas interaction parameters are available. However, besides the recombination coefficient data, the KMC solution embeds more reacting kinetics of the surface reaction system in the catalytic model, strengthening the physical support of the viscous wall boundary description in CFD.



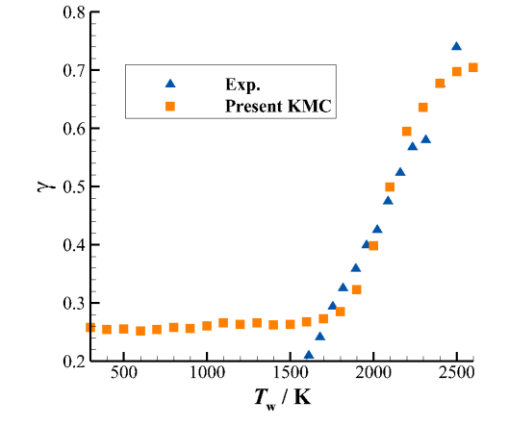


Figure 8 - Recombination coefficients of nitrogen atoms on Pt surface

Figure 9 - Recombination coefficients of nitrogen atoms on the W surface

Recombination of oxygen atoms plays a significant role in aerodynamic heating on silica-based thermal protection materials[51]. As a result, an amount of research on the heterogeneous catalysis behavior of oxygen atoms on these materials has been carried out, including experimental[10, 11]

and theoretical models [52]. However, due to the complexity of material atomic structures, huge uncertainties in the recombination coefficients of oxygen atoms on silica-based materials still exist. Gas-solid interaction parameters of silica-based material were selected from early research according to Refs. [17, 47, 53, 54], which have been listed in Table 3. Using the parameters in Table 3, the rate constant of every reaction step can be calculated by Eqs.(21-23).

$$k_{\rm ER} = C_{\rm ER} \times e^{-\frac{E_{\rm ER}}{k_{\rm B}T_{\rm w}}} \tag{21}$$

$$k_{\rm LH} = (u_{\rm D} \times e^{-\frac{E_{\rm D}}{k_{\rm B}T_{\rm w}}}) \times (C_{\rm LH} \times e^{-\frac{E_{\rm LH}}{k_{\rm B}T_{\rm w}}})$$
 (22)

$$k_{\mathrm{Td}} = U_{\mathrm{Td}} \times e^{-\frac{E_{\mathrm{Td}}}{k_{\mathrm{B}}T_{\mathrm{W}}}} \tag{23}$$

Table 3 Parameter values of four-step reaction rate constants on silica-based material

Parameters	$k_{\mathrm{Ad}}$	S	$C_{\rm ER}$	$C_{LH}$	$\pmb{u}_{ ext{D}}$	$oldsymbol{\mathit{U}}_{\mathrm{Td}}$	$E_{ m ER}$	$E_{\scriptscriptstyle  m D}$	$E_{ m LH}$	$E_{\mathrm{Td}}$
values	1	$1 \times 10^{18} / m^2$	0.6	0.5	1×10 <sup>13</sup>	5×10 <sup>14</sup>	0.149eV	1.46eV	0.25eV	3.0eV

A comparison of oxygen atoms' recombination coefficients from the present KMC simulation and experimental data[10-13] is shown in Figure 10. Experimental tested materials include quartz and RCG. Figure 10 illuminates that the results of the present KMC method are of the same magnitude and temperature-dependent trend as that of experimental data. However, because of uncertainties in material properties, there are wide differences between different experimental results and between KMC simulation and experimental data.

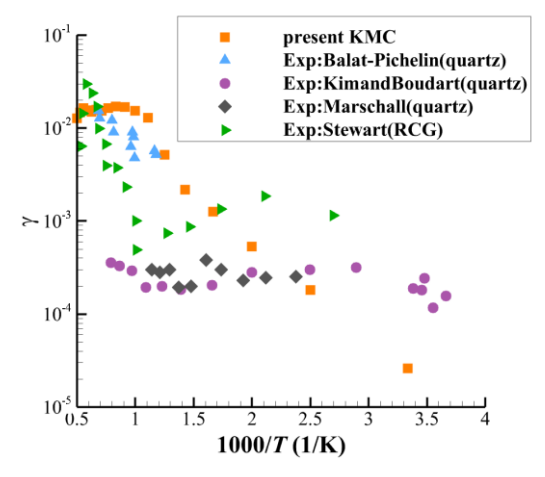


Figure 10 - Recombination coefficients of oxygen atoms on silica-based material surface

## 3.2 Flow field and aerodynamic heating of CFD simulation

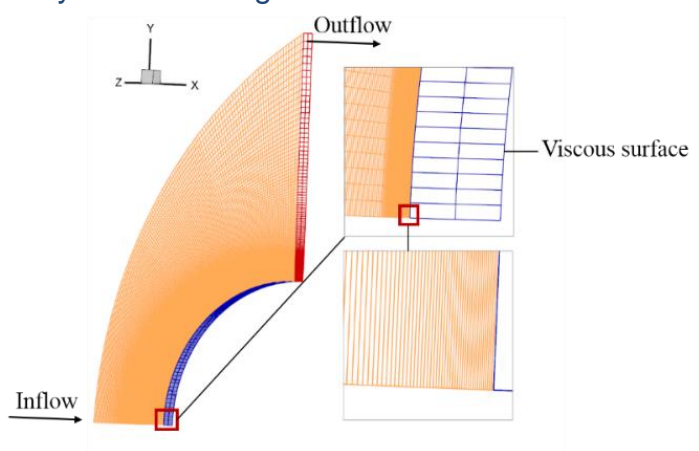


Figure 11 - CFD grids of flow field zone around a 2D cylinder

RUN75 experiment, which focused on the heat transfer rate on the catalytic cylinder surface, was conducted in the LENS wind tunnel[6]. CFD simulation under the same freestream conditions was

done to verify the reliability of CAPTER. The grid of the fluid zone around the 8.9-cm cylinder is shown in Figure 11, of which the first grid layer in the surface normal direction is  $1.0 \times 10^{-6}$  m high. The numbers of nodes in tangential and normal directions are 160 and 240 respectively. The 2D fluid zone in the XOY plane is extended to two grid layers in the Z direction. The fluid zone is divided into 16 blocks. Grids in Figure 11 are fine enough to capture the position of the shock wave and grids near the viscous wall are fine enough to capture the temperature gradient in the thermal boundary layer. Grid independence has been certificated in the author's former work [55]. Freestream conditions of the RUN75 experiment are listed in Table 4. The surface temperature was set to be 300K.

**Table 4** Freestream conditions of experiment RUN75 in LENS wind tunnel[6]

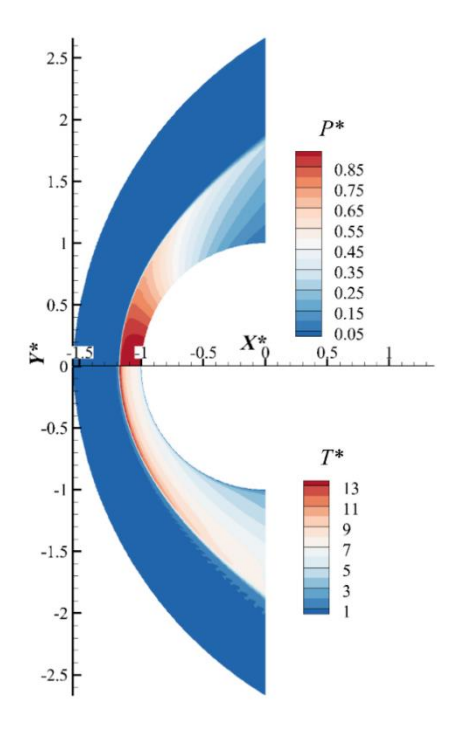
Freestream parameters	Value
Density, kg/m <sup>3</sup>	0.00047
Speed, m/s	7105
Temperature, K	1070
Mach number	11.1
Species mass fraction	$c_{O_2} = 0.23$ , $c_{N_2} = 0.77$

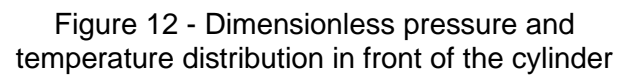
Temperature and pressure fields under freestream conditions shown in Table 4 are given in Figure 12. The viscous wall is fully catalytic (FC) in this case. Coordinates  $X^*$  and  $Y^*$  are dimensionless using cylinder radius. Dimensionless pressure and temperature are defined as

$$P^* = \frac{P}{\rho_{\infty} V_{\infty}^2} \tag{23}$$

$$T^* = \frac{T}{T_{co}} \tag{24}$$

After the shock wave in front of the cylinder surface, pressure increases sharply due to the decrease in velocity. Near the stagnation point, most dynamic pressure is converted to static pressure. While gas temperature reaches the highest at the position of the shock wave, then decreases gradually in the shock layer. This is caused by the dissociation of molecular species.





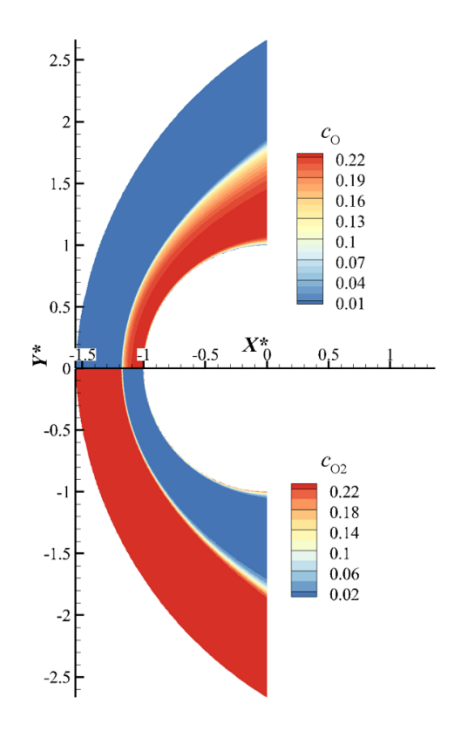


Figure 13 - Mass fractions of oxygen atoms and molecules in the flow field

Figure 13 presents mass fractions of oxygen molecules and atoms in the flow field around the cylinder. Figure 13 reveals the dissociation from molecules to atoms in the shock layer. Before reaching the shock wave, the air keeps its initial species components and there are no atomic species. Heating by high temperature in the shock wave, nearly all molecules are dissociated into atoms. With the variety of local temperatures and species concentrations, the homogeneous reaction occurs in the shock layer. Near the surface, the gas temperature is too low to keep the atomic environment. On the surface, due to fully catalytic properties, all atoms recombine as molecules. As a result, the concentration of atoms decreases in the vicinity of the surface, while that of molecules increases.

Molar fractions of five gas species on the stagnation line calculated by CAPTER were compared with that calculated by DPLR, which has been proven to be effective in simulating chemical reacting flow [56]. As shown in Figure 14(a) and (b), both DPLR and CAPTER can capture the dissociation of molecules after the shock wave and recombination of atoms near the cold surface. The position of the shock wave predicted by CAPTER is similar to that of DPLR as well. Little difference in molar fractions of nitrogen atoms and molecules is caused by the selection of gas models.

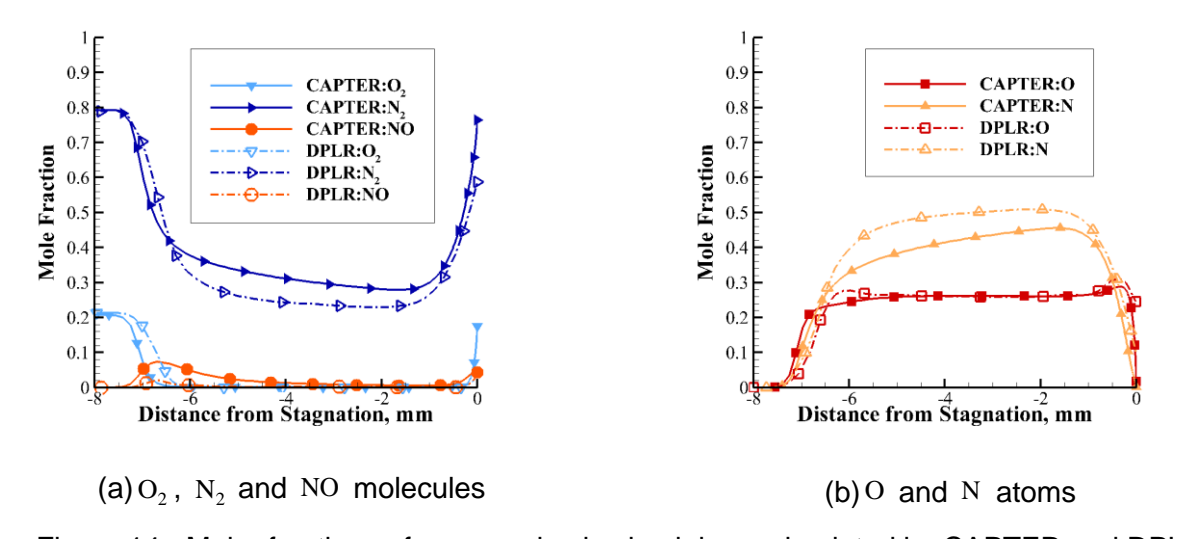


Figure 14 - Molar fractions of gas species in shock layer simulated by CAPTER and DPLR To consider the surface catalysis effect in CFD prediction of surface heat transfer rate, a straightforward way is to specify recombination coefficients of atomic species on viscous wall boundary. Two extremes of this method are the non-catalytic (NC) surface and FC surface. By specifying different finite recombination coefficients of oxygen atoms in CAPTER, heat transfer rate on the cylinder surface can be obtained. Figure 15 indicates that NC and FC conditions result in the minimum and maximum surface heat transfer rates. Heat transfer rates on finite-catalytic surfaces are located between these two extremes. With the increase of the recombination coefficient, the heat transfer rate increases gradually. The above phenomena reflect the fact that CAPTER can predict the chemical non-equilibrium flow field and the range of surface heat transfer rate. However, it's still difficult for a CFD solver to accurately handle mass and heat transfer rate on a catalytic surface.

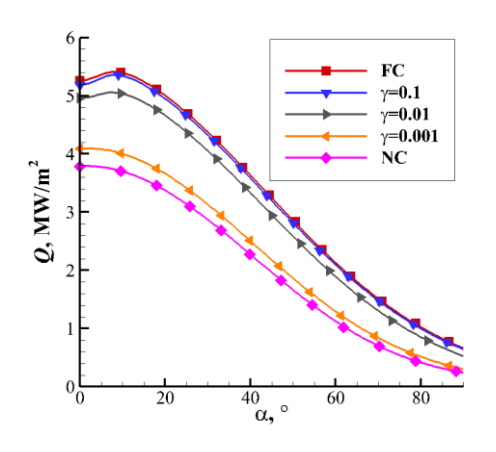


Figure 15 - Heat transfer rates under different recombination coefficients

## 3.3 Aerodynamic heating prediction of KMC embedded CFD method

KMC-embedded CFD simulation was carried out on the same 2D cylinder under freestream conditions in Table 4. The surface material is Pt, of which the rate-related parameters were obtained from Ref. [48]. Parallel KMC-embedded CFD computation used 16 CPU cores in this case and one core answered for one grid block. On the viscous wall boundary of every block, KMC simulations, including heterogeneous catalysis simulation of oxygen and nitrogen atoms on the Pt surface, were operated on the four vertices, as shown in Figure 16. Recombination coefficients of other grid nodes on this surface were obtained by interpolation method in section2.4.

Due to the random characteristic of the KMC method, heat transfer results of the KMC-embedded CFD method fluctuate with CFD iterations. As shown in Figure 7, recombination coefficients under a single condition would fluctuate with KMC iterations. Therefore, another KMC simulation under the same thermochemical condition couldn't get a duplicate recombination coefficient. What's more, the thermochemical environment of the same grid node won't be the same for different CFD iterations. Little difference in recombination coefficient (results of KMC simulation) will lead to light fluctuation of species concentration on the viscous wall boundary (CFD simulation), further changing the thermochemical condition of KMC simulation in the next CFD iteration step. Monitoring the maximum heat transfer rate,  $Q_{\text{max}}$ , on the Pt cylinder surface, fluctuation can be seen in Figure 17. Average of  $Q_{\text{max}}$  during these 400 iteration steps in Figure 17 is 5.109 MW/m². Maximum and minimum of  $Q_{\text{max}}$  are 5.139 MW/m² and 5.080 MW/m² respectively, resulting in a largest relative fluctuation of 1.15%.

are 5.139 MW/m<sup>2</sup> and 5.080 MW/m<sup>2</sup> respectively, resulting in a largest relative fluctuation of 1.15%. Compared with the strong uncertainty of heat transfer rate caused by catalytic property in Figure 15, this fluctuation is negligible.

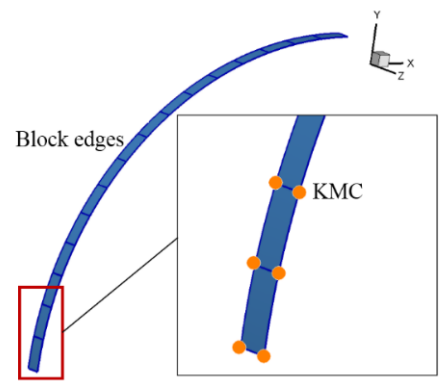
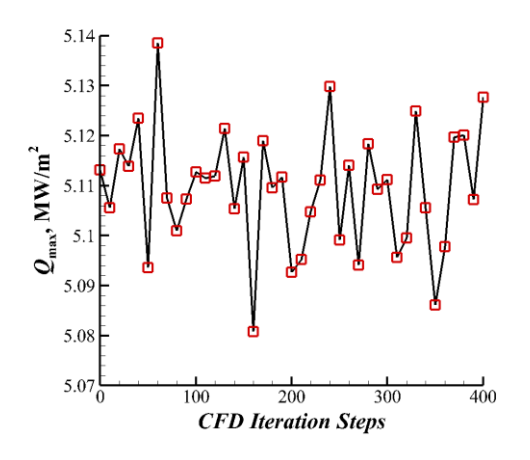


Figure 16 - Locations to carry out KMC simulation on the viscous wall of the 2D cylinder



CFD/KMC: Pt
NC
Exp.1
Exp.2
Exp.3

Figure 17 - Fluctuation of maximum heat transfer rate with iteration steps

Figure 18 - Heat transfer rate obtained by KMC embedded CFD method

The surface heat transfer rate Q on the cylinder of Pt material obtained by the KMC-embedded CFD method is shown in Figure 18. Compared with the experimental heat transfer rate on a stainless

steel surface, Q on Pt surface is a little higher. However, compared to the uncertainty caused by the NC and FC hypothesis, the results of the KMC-embedded CFD method are much more determinate. The most significant advantage of this simulation is that KMC simulation (atomic scale) involves chemical kinetics and material thermal physics in CFD prediction (continuum) of surface heat transfer. As a result, KMC simulation can provide a local thermochemical-dependent recombination coefficient for CFD. Heat transfer rate is influenced by the surface material, so accurate thermophysical properties of TPS materials are necessary to accurately predict heat transfer rate with heterogeneous catalysis effect.

Under the catalysis of Pt material, atom species distribution near the surface is much different from that of NC and FC surfaces. Figure 19(a) and (b) report mass fractions of dissociated oxygen atoms and nitrogen atoms on the stagnation line respectively. Little oxygen atoms recombine on the NC surface, while all of them recombine on the FC surface. Part of oxygen atoms recombine on the finite rate catalytic material, Pt. A similar trend can be found in the mass fraction variety of nitrogen atoms.

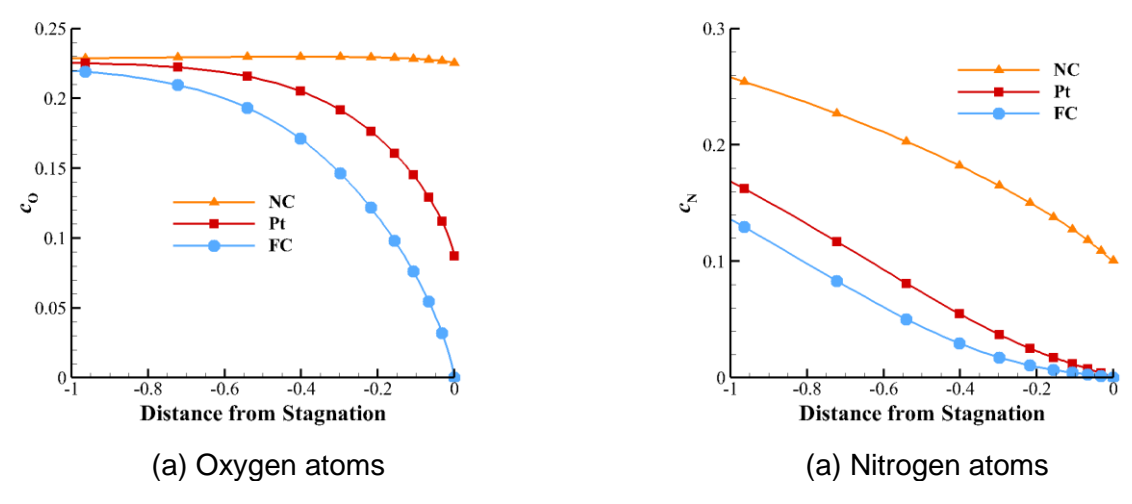


Figure 19 - Mass fraction of dissociated atoms near the surface

Furthermore, the compromise of efficiency and accuracy is an eternal dilemma in the numerical simulation of physical phenomena. Although prediction determinacy is improved by embedding KMC into CFD methods, the time cost is sharply increased as well. For the simulation of the present 2D cylinder, the computational time of a single iteration step increases from 0.5 s (CFD) to more than 800 s (CFD-KMC), indicating more than 1000 times increase in time cost. This is caused by the truth that KMC simulation on a 40\*40 lattice costs about 200s and one surface has 4 vertices to operate KMC simulation. Because one CPU core answers for four KMC simulations in KMC embedded CFD simulation, the time consumption of one iteration is about 800 s. Fortunately, it's not necessary to calculate the flow field by the KMC-embedded CFD method from the initial state. A steady flow field can be obtained from CFD simulation with FC or NC surface. Based on this flow field, iteration steps of the KMC-embedded CFD simulation will reduce sharply, further saving time costs. In the future, if machine learning methods can be introduced into the coupling between KMC and CFD, the magnitude of time consumption will be reduced significantly.

## 4. Conclusions

Based on a four-step heterogeneous catalysis mechanism, a catalytic viscous wall boundary model using the KMC method was constructed and coupled into the chemical non-equilibrium CFD solver by bilinear interpolation. The KMC-embedded CFD method was applied in heat transfer rate calculation on a 2D cylinder surface in high-speed flow. Conclusions can be drawn as:

- (1) The KMC model has been proven to be useful in calculating the recombination coefficient of atoms on the condition that gas-solid interaction parameters are available. The KMC-based catalytic model takes both local thermochemical conditions and gas-solid interaction kinetics into consideration, resulting in a physics-dependent catalytic model.
- (2) Based on known surface reaction parameters, the KMC-embedded CFD method can obtain local deterministic recombination coefficient and heat transfer rate. KMC simulation provides the intrinsic

mechanism of heterogeneous catalysis in the macroscopic calculation of heat and mass transfer on the gas-solid interface. Therefore, the macroscopic solution embeds more physical information. However, calculation efficiency becomes a limitation of the KMC-embedded CFD method.

In the future, effort should be put into two aspects. First, the precise description of reaction trajectory and accurate gas-surface interaction parameters on thermal protection materials are of vital importance for more accurate surface mass and heat transfer. This can be realized by microscopic simulations (such as Density Function Theory) and reactor experiments. Secondly, acceleration methods, such as machine learning, should be applied to the coupling between the mesoscale KMC method and CFD, to improve computational efficiency.

## 5. Acknowledgement

This research was supported by the National Key Research and Development Program of China (No. 2019YFA0405202) and the National Natural Science Foundation of China (No. 12072361).

## 6. Contact Author Email Address

Mailto: yxf.2006@tsinghua.org.cn, wdong@sjtu.edu.cn

## 7. Copyright Statement

The authors confirm that they, and/or their company or organization, hold copyright on all of the original material included in this paper. The authors also confirm that they have obtained permission, from the copyright holder of any third party material included in this paper, to publish it as part of their paper. The authors confirm that they give permission, or have obtained permission from the copyright holder of this paper, for the publication and distribution of this paper as part of the ICAS proceedings or as individual off-prints from the proceedings.

### References

- [1] Gui Y. Combined thermal phenomena of hypersonic vehicle. Scientia Sinica Physica, Mechanica & Astronomica, Vol. 49, No. 11, pp 139-53, 2019.
- [2] Anderson J D. Hypersonic and high-temperature gas dynamics. Second edition, American Institute of Aeronautics and Astronautics, Inc., 2009.
- [3] Yang X, Li Q, Du Y, et al. Progress in numerical research on interface heterogeneous catalysis of hypersonic vehicles. Acta Aeronautica et Astronautica Sinica, Vol. 42, No. 12, pp 625908, 2021.
- [4] Herdrich G, Fertig M. Catalysis of Metallic and Ceramic TPS-Materials. Transactions of the Japan Society for Aeronautical and Space Sciences, Space Technology Japan, Vol. 7, No. 26, pp 49-58, 2009.
- [5] Wright M, Edquist K, Tang C, et al. A Review of Aerothermal Modeling for Mars Entry Missions; Proc Conference 48th AIAA Aerospace Sciences Meeting Including the New Horizons Forum and Aerospace Exposition, AIAA 2010-443, 2010.
- [6] MacLean M, Marineau E, Parker R, et al. Effect of Surface Catalysis on Measured Heat Transfer in an Expansion Tunnel Facility; Proc Conference 50th AIAA Aerospace Sciences Meeting including the New Horizons Forum and Aerospace Exposition, Nashville, Tennessee, 2012-0651, pp 2012-0651, 2012.
- [7] Inger G R, Baker R L. Nonequilibrium Viscous Shock-Layer Heat Transfer with Arbitrary Surface Catalycity. Journal of Spacecraft & Rockets, Vol. 42, No. 2, pp 193-200, 2015.
- [8] Yang X, Gui Y, Tang W, et al. Surface Chemical Effects on Hypersonic Nonequilibrium Aeroheating in Dissociated Carbon–Oxygen Mixture. Journal of Spacecraft & Rockets, Vol. 55, No. 3, pp 687-97, 2018.
- [9] Yang X, Gui Y, Xiao G, et al. Reacting gas-surface interaction and heat transfer characteristics for highenthalpy and hypersonic dissociated carbon dioxide flow. International Journal of Heat and Mass Transfer, Vol. 146, No. 2020, pp 118869, 2020.
- [10]Kim Y C, Boudart M. Recombination of O, N, and H atoms on silica. Kinetics and mechanism. Vol. No. 1991.
- [11]Balat-Pichelin M, Badie J M, Berjoan R, et al. Recombination coefficient of atomic oxygen on ceramic materials under earth re-entry conditions by optical emission spectroscopy. Chemical Physics, Vol. 291, No. 2, pp 181-94, 2003.
- [12]Marschall J. Experimental determination of oxygen and nitrogen recombination coefficients at elevated temperatures using laser-induced fluorescence; Proc Conference National Heat Transfer Conference, Baltimore, MD, 97-3879, 1997.
- [13]Stewart D A. Surface Catalysis and Characterization of Proposed Candidate TPS for Access-to-Space Vehicles. United States: NASA, 1997.
- [14]Bedra L, Balat-Pichelin M J H. Comparative modeling study and experimental results of atomic oxygen recombination on silica-based surfaces at high temperature. Aerospace Science and Technology, Vol. 9, No. 4, pp 318-28, 2005.
- [15]Norman P, Schwartzentruber T, Cozmuta I. Modeling Air-SiO2 Surface Catalysis Under Hypersonic Conditions with ReaxFF Molecular Dynamics; Proc Conference 10th AIAA/ASME Joint Thermophysics and Heat Transfer Conference, Chicago, Illinois, 2010-4320, pp 2010-4320, 2010.
- [16]Norman P, Schwartzentruber T, Cozmuta I. A Computational Chemistry Methodology for Developing an Oxygen-Silica Finite Rate Catalytic Model for Hypersonic Flows; Proc Conference 42nd AIAA Thermophysics Conference, Hawaii, 2011-3644, pp 2011-3644, 2011.
- [17]Norman P, Schwartzentruber T. A Computational Chemistry Methodology for Developing an Oxygen-Silica Finite Rate Catalytic Model for Hypersonic Flows: Part II; Proc Conference 43rd AIAA Thermophysics Conference, New Orleans, Louisiana, AIAA 2012-3097, 2012.
- [18] Valentini P, Schwartzentruber T E, Cozmuta I. Molecular dynamics simulation of O2 sticking on Pt(111) using the ab initio based ReaxFF reactive force field. Journal of Chemical Physics, Vol. 133, No. 8, pp 718, 2010.
- [19] Valentini P, Schwartzentruber T, Cozmuta I. ReaxFF atomic-level simulation of catalytic processes on platinum; Proc Conference 42nd AIAA Thermophysics Conference, Honolulu, Hawaii, 2011-3645, 2011.
- [20]Buchachenko A A, Kroupnov A A, Kovalev V L. First-principle study of atomic oxygen and nitrogen adsorption on (111)  $\beta$ -cristobalite as a model of thermal protection coverage. Acta Astronautica, Vol. 100, No. pp 40-6, 2014.
- [21]Buchachenko A A, Kovalev V L, Krupnov A A. Rate coefficients of the elementary stages of heterogeneous catalytic recombination of dissociated air on thermal-protective coatings. Fluid Dynamics, Vol. 50, No. 3, pp 453-62, 2015.
- [22]Buchachenko A A, Kroupnov A A, Kovalev V L. Elementary stage rate coefficients of heterogeneous catalytic recombination of dissociated air on thermal protective surfaces from ab initio approach. Acta Astronautica, Vol. 113, No. 2015, pp 142-8, 2015.
- [23]Cui Z, Zhao J, Yao G, et al. Competing effects of surface catalysis and ablation in hypersonic reentry aerothermodynamic environment. Chinese Journal of Aeronautics, Vol. 35, No. 10, pp 11, 2022.

- [24] Jansen A P J. An Introduction to Kinetic Monte Carlo Simulations of Surface Reactions. Springer, 2012.
- [25]Papanikolaou K G, Stamatakis M. Toward the accurate modeling of the kinetics of surface reactions using the kinetic Monte Carlo method [M]//GRAMMATIKOPOULOS P. Computational Modelling of Nanomaterials. 2020.
- [26] Jørgensen M, Grönbeck H. Scaling Relations and Kinetic Monte Carlo Simulations To Bridge the Materials Gap in Heterogeneous Catalysis. ACS Catalysis, Vol. 7, No. 8, pp 5054-61, 2017.
- [27]Mikael L, V. S N. KMCLib: A general framework for lattice kinetic Monte Carlo (KMC) simulations. Computer Physics Communications, Vol. 185, No. 9, pp 2340-9, 2014.
- [28]Mikael L, V. S N. KMCLib 1.1: Extended random number support and technical updates to the KMCLib general framework for kinetic Monte-Carlo simulations. Computer Physics Communications, Vol. 196, No. pp 611-3, 2015.
- [29]Hoffmann M J, Matera S, Reuter K. kmos: A lattice kinetic Monte Carlo framework. Computer Physics Communications, Vol. 185, No. 7, pp 2138-50, 2014.
- [30] Jørgensen M, Grönbeck H. Monte Coffee: A programmable kinetic Monte Carlo framework. The Journal of Chemical Physics, Vol. 149, No. 11401, 2018.
- [31]Dooling D J, Broadbelt L J. Generic Monte Carlo Tool for Kinetic Modeling. Industrial & Engineering Chemistry Research, Vol. 40, No. 2, pp 522-9, 2001.
- [32] Andersen M, Panosetti C, Reuter K. A Practical Guide to Surface Kinetic Monte Carlo Simulations. Front Chem, Vol. 7, No. pp 202, 2019.
- [33] Guerra V, Loureiro J. Dynamical Monte Carlo simulation of surface atomic recombination. Plasma Sources Science and Technology, Vol. 13, No. 1, pp 85-94, 2004.
- [34] Fichthorn K A, Weinberg W H. Theoretical Foundations of Dynamic Monte Carlo Simulations. The Journal of Chemical Physics, Vol. 95(2), No. pp 1090-6, 1991.
- [35]Schaefer C, Jansen A P J. Coupling of kinetic Monte Carlo simulations of surface reactions to transport in a fluid for heterogeneous catalytic reactor modeling. Journal of Chemical Physics, Vol. 138, No. 5, pp 054102, 2013.
- [36]Donghai M, Guang L. Effects of heat and mass transfer on the kinetics of CO oxidation over RuO2(110) catalyst. Catalysis Today, Vol. 165, No. 1, pp 56-63, 2011.
- [37]Matera S, Meskine H, Reuter K. Adlayer inhomogeneity without lateral interactions: Rationalizing correlation effects in CO oxidation at RuO2(110) with first-principles kinetic Monte Carlo. Journal of Chemical Physics, Vol. 134, No. 6, pp 064713, 2011.
- [38]Hess F, Farkas A, Seitsonen A P, et al. "First-principles" kinetic Monte Carlo simulations revisited: CO oxidation over RuO2 (110). Journal of computational chemistry, Vol. 33, No. 7, pp 757-66, 2012.
- [39]Schlexer P. Computational Modeling in Heterogeneous Catalysis. Reference Module in Chemistry, Molecular Sciences and Chemical Engineering, Vol. No. 2017.
- [40] Thoemel J, Lukkien J J, Chazot O. A Multiscale Approach for Building a Mechanism Based Catalysis Model for High Enthalpy Carbon Dioxide Flow; Proc Conference 39th AIAA Thermophysics Conference, Miami, FL, 2007-4399, pp 2007-4399, 2007.
- [41]Gui Y, Liu L, Dai G, et al. Research status of hypersonic vehicle fluid-thermal-solid coupling and software development. Acta Aeronautica et Astronautica Sinica, Vol. 38, No. 7, pp 020844, 2017.
- [42] Park C, Jaffe R L, Partridge H. Chemical-Kinetic Parameters of Hyperbolic Earth Entry. Journal of thermophysics and heat transfer, Vol. 15, No. 1, pp 76-90, 2001.
- [43]Gupta R N, Yos J M, Thompson R A. A review of reaction rates and thermodynamic and transport properties for the 11-species air model for chemical and thermal nonequilibrium calculations to 30000K, 1990.
- [44]Kim J G, Jo S M. Modification of chemical-kinetic parameters for 11-air species in re-entry flows. International Journal of Heat and Mass Transfer, Vol. 169, No. 10, pp 120950, 2021.
- [45]Yang X, Radespiel R. Longitudinal aerodynamic performance of the Apollo entry capsule near transonic speeds. Journal of Spacecraft and Rockets, Vol. 54, No. 5, pp 1100-9, 2017.
- [46]Yang X, Xiao G, Du Y, et al. Heat Transfer with Interface Effects in High-Enthalpy and High-Speed Flow: Modelling Review and Recent Progress. Applied Thermal Engineering, Vol. 195, No. pp 116721, 2021.
- [47]Li K, Liu J, Liu W. A new surface catalytic model for silica-based thermal protection material for hypersonic vehicles. Chinese Journal of Aeronautics, Vol. 28, No. 5, pp 1355-61, 2015.
- [48]Barbato M, Reggiani S, Bruno C, et al. Model for Heterogeneous Catalysis on Metal Surfaces with Applications to Hypersonic Flows. Journal of Thermophysics and Heat Transfer, Vol. 14, No. 3, pp 412-20, 2000.
- [49]Armenise I, Barbato M, Capitelli M, et al. State-to-State Catalytic Models, Kinetics, and Transport in Hypersonic Boundary Layers. Journal of Thermophysics and Heat Transfer, Vol. 20, No. 3, pp 465-76, 2006.
- [50] Halpern B, Rosner D E. Chemical energy accommodation at catalyst surfaces. Flow reactor studies of the

- association of nitrogen atoms on metals at high temperatures. Journal of the Chemical Society Faraday Transactions, Vol. 74, No. pp 1883-912, 1978.
- [51] Seward W A, Jumper E J. Model for oxygen recombination on silicon-dioxide surfaces. Journal of Thermophysics and Heat Transfer, Vol. 5, No. 3, pp 284-91, 1991.
- [52] Jumper E J, Seward W A. Model for oxygen recombination on reaction-cured glass. Journal of Thermophysics and Heat Transfer, Vol. 8, No. 3, pp 460-5, 1994.
- [53]Shiozaki S, Sakiyama Y, Takagi S, et al. Multiscale Analysis of Heterogeneous Catalysis on a Silica Surface; Proc Conference 46th AIAA Aerospace Sciences Meeting and Exhibit, 2008.
- [54] Daniil M, Carlos T, Vasco G. Deterministic and Monte Carlo methods for simulation of plasma-surface interactions. Plasma Processes & Polymers, Vol. 14, No. 1-2, pp 1600175, 2017.
- [55]Li Q, Yang X, Dong W, et al. Numerical Simulation on Influence of Adsorption on Surface Heterogeneous Catalysis Process of Hypersonic Vehicle. Journal of Shanghai Jiao Tong University, Vol. 55, No. 11, pp 1352-61, 2021.
- [56]MacLean M, Holden M, Wadhams T, et al. A Computational Analysis of Thermochemical Studies in the LENS Facilities; Proc Conference 45th AIAA Aerospace Sciences Meeting and Exhibit, Nevada, 2007-121, 2007.